AGU PUBLICATIONS

Geophysical Research Letters

RESEARCH LETTER
10.1002/2015GL064793

Key Point:
- Stress drop and rupture velocity are anticorrelated

Supporting Information:
- Supporting Information S1

Correspondence to:
M. Causse,
mathieu.causse@ujf-grenoble.fr

Citation:
Causse, M., and S. G. Song (2015), Are stress drop and rupture velocity of earthquakes independent? Insight from observed ground motion variability, *Geophys. Res. Lett.*, *42*, doi:10.1002/2015GL064793.

Received 3 JUN 2015
Accepted 19 AUG 2015
Accepted article online 22 AUG 2015

Are stress drop and rupture velocity of earthquakes independent? Insight from observed ground motion variability

Mathieu Causse[1] and Seok Goo Song[2]

[1]ISTerre, IFSTTAR, University Grenoble Alpes, Grenoble, France, [2]Earthquake Research Center, Korea Institute of Geoscience and Mineral Resources, Daejeon, South Korea

Abstract We demonstrate that the variability of the peak ground acceleration (PGA) generated by earthquakes can be simply related to the variability of stress drop ($\Delta\tau$), rupture velocity (V_r) and their correlation. By compiling recent observations of variability of $\Delta\tau$ and V_r, we show that the hypothesis of independence between $\Delta\tau$ and V_r leads to an overestimation of the PGA variability. We suggest that $\Delta\tau$ and V_r must be anticorrelated so as to match recent observations of PGA variability.

1. Introduction

Earthquake source studies reveal that stress drop ($\Delta\tau$) and rupture velocity (V_r) of earthquakes can vary significantly from one event to the other [e.g., *Allmann and Shearer,* 2009; *Heaton*, 1990]. Defining the natural randomness of the source process, which is the variability in repeated ruptures of a given magnitude on the same fault, is a key issue in seismic hazard assessment because it is needed for proper estimation of the variability in ground motion predictions [*Anderson and Brune,* 1999]. The main question is what fraction of the observed dispersion actually arises from the source process.

Recently, *Cotton et al.* [2013] have pointed out that the large scatter of stress drop values obtained in analyses of earthquake spectra may essentially reflect uncertainties in corner frequency (f_c) estimates and lead to strongly overestimated variability of ground motion. But another explanation lies in the assumed relationship between corner frequency and stress drop, which is commonly based on a simple *Brune's* [1970] source model. This model assumes that f_c scales with the inverse of the rupture dimension and that the rupture velocity is constant. For a given seismic moment, it implies that $f_c \propto \Delta\tau^{1/3}$. *Kaneko and Shearer* [2015] have shown that considering various rupture velocities values in a *Brune* [1970] like source model can explain most of the stress drop scattering. A probably more realistic assumption that f_c scales with the inverse of the rupture duration [e.g., *Kanamori and Rivera*, 2004], which gives

$$f_c \propto V_r \Delta\tau^{1/3} \tag{1}$$

Assuming that the displacement spectrum follows a f^{-2} decay beyond the corner frequency [e.g., *Brune*, 1970], *McGuire and Hanks* [1980] obtained that

$$a_{RMS} \propto f_c^{5/2} \tag{2}$$

Using the theory of random vibration, *Hanks and McGuire* [1981] showed that PGA and a_{RMS} are linked by the following relationship: $\mathrm{PGA} \propto a_{RMS}\sqrt{2\ln(2f_{\max}/f_c)}$. Following the approximation proposed by *Boore* [1983], the scaling of PGA with f_c is then given by

$$\mathrm{PGA} \propto f_c^{2.4}$$

Thus, from equation (1), we obtain that $\mathrm{PGA} \propto V_r^{2.4}\Delta\tau^{0.8}$. Since PGA follows a lognormal distribution [e.g., *Bommer et al.,* 2004], we consider the logarithm values:

$$\ln(\mathrm{PGA}) = 2.4\ln(V_r) + 0.8\ln(\Delta\tau) + c \tag{3}$$

where c is constant. It is clear from equation (3) that for a given seismic moment, the PGA variability depends on the variability of V_r and $\Delta\tau$ and their correlation. The standard deviation of ln(PGA) is given by

$$\sigma_{\ln(\mathrm{PGA})} = \sqrt{5.76\sigma_{\ln(Vr)}{}^2 + 0.64\sigma_{\ln(\Delta\tau)}{}^2 + 3.84\sigma_{\ln(Vr)} \cdot \sigma_{\ln(\Delta\tau)} \cdot \mathrm{CORR}_{\ln}} \tag{4}$$

where $\mathrm{CORR}_{\ln}$ is the coefficient of correlation between $\ln(V_r)$ and $\ln(\Delta\tau)$.

Table 1. Stress Drop Variability Inferred From Various Recent Studies[a]

Reference	Data Type	Data Set	Estimated Parameter	Definition of Inferred Stress Drop	Inferred Stress Drop Variability $\sigma_{\ln(\Delta\tau)}$
Shaw [2013]	Surface slip-length observations	37 strike-slip events ($M > 6$)	D_{mean}/L	$\Delta\tau_M$	0.7
Manighetti et al. [2007]	Surface slip-length observations and finite-source models	~250 continental earthquakes ($M > \sim 6$)	D_{max}/L	$\Delta\tau_M$	0.9
Mai and Beroza [2000]	Finite-source rupture models	31 source models of 18 events ($5.5 < M < 8$)	$D_{mean}/L_{eff.}$	$\Delta\tau_M$	0.8
Causse et al. [2014]	Finite-source rupture models	31 source models of 21 crustal events ($5.8 < M < 7.6$)	Spatial distribution of stress drop ($\tau_{initial} - \tau_{final}$)	$\Delta\tau_A$	0.7
Baltay et al. [2013][b]	Earthquake spectra	59 events from two earthquake sequences ($3 < M < 7$)	a_{RMS} stress drop	$\Delta\tau_M$	0.9

[a]The considered studies are based on the analysis of global earthquake databases, except the study of *Baltay et al.* [2013], using data of two earthquakes sequences in Japan (2004 Chuetsu and 2008 Iwate-Miyagi events). D_{mean} and D_{max} denote the average and the maximum slip, respectively. $L_{eff.}$ is the effective rupture length, as proposed by *Mai and Beroza* [2000] to characterize the rupture length in finite-source rupture models. $\Delta\tau_A$ and $\Delta\tau_M$ refer to different definitions of the stress drop, described in equations (5) and (6).
[b]Note that *Baltay et al.* [2013] use the relationship of *Hanks* [1979] to infer the a_{RMS} stress drop, in which stress drop scales with $\sqrt{f_c}$.

This article aims to investigate the dependency between $\Delta\tau$ and V_r. Due to the limited number of independent direct estimates of $\Delta\tau$ and V_r, this question has remained open but is of fundamental interest not only for understanding how earthquake rupture propagates but also for improving ground motion predictions. We tackle this issue by bringing face to face recent observations of variability of $\Delta\tau$, V_r, and the variability of event term for PGA ground motion. We do this using the simple relationship proposed in equation (4). The validity of this relationship is next checked in the case of heterogeneous ruptures, deploying ground motion simulations performed from 1-D stochastic source models.

2. Observed Variability of Stress Drop, Rupture Velocity, and Ground Motion

2.1. Stress Drop

Observations suggest that stress drop is spatially variable [e.g., *Bouchon*, 1997] and hence should be characterized by a distribution. It raises the questions of how to define the average stress drop and what value of $\Delta\tau$ should be considered in equation (1). *Noda et al.* [2013] compared different stress drop measures in 2-D stochastic source models with heterogeneous stress drop distributions. They showed that the average of the local stress drop, defined as

$$\Delta\tau_A = 1/S\int_S(\tau_i - \tau_f)\mathrm{d}S \tag{5}$$

where S is the surface of the rupture area and $\tau_i - \tau_f$ is difference of stress level before and after the rupture, is consistent with stress drop measure based on seismic moment (M_0) and shape of rupture area, given by [e.g., *Kanamori and Anderson*, 1975]

$$\Delta\tau_M = CM_0/S^{3/2} = C\mu D/\sqrt{S} \tag{6}$$

where C depends on the rupture area shape, D is the average slip on surface S, and μ is the rigidity. $\Delta\tau_M$ is classically deduced by modeling earthquake spectra, but also from observations of surface ruptures and finite-source rupture models. $\Delta\tau_A$ can be derived from finite-source rupture models only, because it requires the spatial distribution of stress drop.

Here we analyze the variability of stress drop ($\Delta\tau_M$ or $\Delta\tau_A$) as reported in some recent studies from various types of data (Table 1). The stress drop values are generally found to follow a lognormal distribution, and so the variability is thus defined as the standard deviation of the stress drop natural logarithm residuals around the median, for a given seismic moment ($\sigma_{\ln(\Delta\tau)}$). The values reported in Table 1 range from 0.7 to 0.9. The associated uncertainties are examined in section 5. Note that we have excluded studies based on corner frequency estimates of earthquake spectra, which generally lead to large stress drop variability on the order of $\sigma_{\ln(\Delta\tau)} \sim 1.5$ [*Cotton et al.*, 2013]. One reason may be that stress drop is then strongly sensitive to uncertainties in the corner frequency estimates, because it scales with the cubed corner frequency.

Table 2. Values of the Between-Event Variability of PGA Reported by Some Recent Ground Motion Prediction Equations (GMPEs) for Crustal Events[a]

Ground Motion Prediction Equation	Between-Event Variability of PGA
Campbell and Bozorgnia [2014] (*M* 6)	0.32
Campbell and Bozorgnia [2014] (*M* 7)	0.32
Boore et al. [2014] (*M* 6)	0.35
Boore et al. [2014] (*M* 7)	0.35
Chiou and Youngs [2014] (*M* 6)	0.31
Chiou and Youngs [2014] (*M* 7)	0.26
Abrahamson et al. [2014] (*M* 6)	0.42
Abrahamson et al. [2014] (*M* 7)	0.36
Akkar and Bommer [2010]	0.23

[a]All GMPEs use the Next Generation Attenuation-West2 database, except *Akkar and Bommer* [2010], who use a European database.

However, we have included the study of *Baltay et al.* [2013], who obtained $\sigma_{\ln(\Delta\tau)} = 0.9$ using the relationship of *Hanks* [1979] to infer the a_{RMS} stress drop, in which stress drop scales with $\sqrt{f_c}$.

2.2. Rupture Velocity

Rupture velocity values reported in source studies mainly range between $0.65V_s$ and $0.85V_s$ [e.g., *Heaton*, 1990]. Dynamic rupture simulations, however, show that in-plane shear cracks can propagate at supershear speeds, that is, faster than V_s, up to V_p [e.g., *Andrews*, 1976]. This is supported by several observations [e.g., *Bouchon et al.*, 2001; *Yue et al.*, 2013], but only seven occurrences of supershear speed have been reported so far. The speed range between $V_{Raiyleigh} \sim 0.9V_s$ and V_s is in principle "forbidden", because the energy consumed at crack tip would become negative. *Bizzarri and Das* [2012] showed that 3-D ruptures can actually pass through this forbidden zone but only transiently.

2.3. Between-Event Variability of Ground Motion (PGA)

Ground motion prediction equations are commonly used in seismic hazard studies to predict a ground motion indicator (e.g., PGA) from basic parameters such as magnitude, distance, and site category. They are developed by means of regression techniques using databases of earthquake strong motion recordings. The average residual for any one earthquake, known as the "between-event" residual, "reflects the influence of factors such as stress drop and variation of slip in space and time that are not captured by the inclusion of magnitude, style of faulting, and source depth" [*Al-Atik et al.*, 2010]. In this framework, the variability of these between-event residuals of ground motion represents the variability due to source effects, averaged over all stations that record that event, and hence all represented azimuths. In most of the studies, the determined between-event variability is not "single path" because the considered data set mixes earthquakes from different source areas and recorded at different sites. As such, the between-event variability represents an upper bound of the ground motion variability due to source randomness. The values of the between-event variability of PGA recently reported for $M \geq 6$ crustal events are between ~0.25 and ~0.4 (Table 2).

3. Inferred Joint Distributions of Rupture Velocity and Stress Drop

In this section we consider probability density functions of $\Delta\tau$ and V_r consistent with the above mentioned source observations. Next we deduce the standard deviation of PGA assuming various levels of correlation between $\Delta\tau$ and V_r by using the simple relationship of equation (4) and compare it with the observed between-event variability of PGA.

Figure 1 displays the PGA variability computed from equation (4) as a function of $\sigma_{\ln(\Delta\tau)}$, assuming that $\Delta\tau$ follows a lognormal distribution. Two types of distribution are considered for the rupture velocity. First, we assume that the V_r values follow a uniform distribution in the range $[0.65V_s–0.85V_s]$, with $V_s = 3500$ m/s (continuous lines). In order to account for a potentially larger variability of V_r and not to exclude supershear ruptures, we consider a second distribution in which 98% of the V_r values are uniformly distributed in the range $[0.65V_s–0.85V_s]$ and 2% are uniformly distributed in the range $[V_s–V_p]$ (dashed lines). We assume that $V_p \sim 1.7V_s$, that is, a Poisson ratio of ~0.25. These two distributions lead to $\sigma_{\ln(Vr)} = 0.08$ and $\sigma_{\ln(Vr)} = 0.14$, respectively (details on the computation of $\sigma_{\ln(Vr)}$ can be found in Text S1 in the supporting information). In order to visualize the effect of the variability of V_r on the PGA variability, Figure 1 also shows $\sigma_{\ln(PGA)}$ computed for a constant rupture velocity which corresponds to $\sigma_{\ln(PGA)} = 0.8\sigma_{\ln(\Delta\tau)}$.

Assuming $\sigma_{\ln(\Delta\tau)} = 0.7$ (Table 1), Figure 1 indicates that when V_r and $\Delta\tau$ are independent (black lines, regardless of the V_r distribution), the resultant $\sigma_{\ln(PGA)}$, near 0.6, would be much larger than the reported between-event variability (indicated in the grey horizontal bar). There are two main hypotheses that can

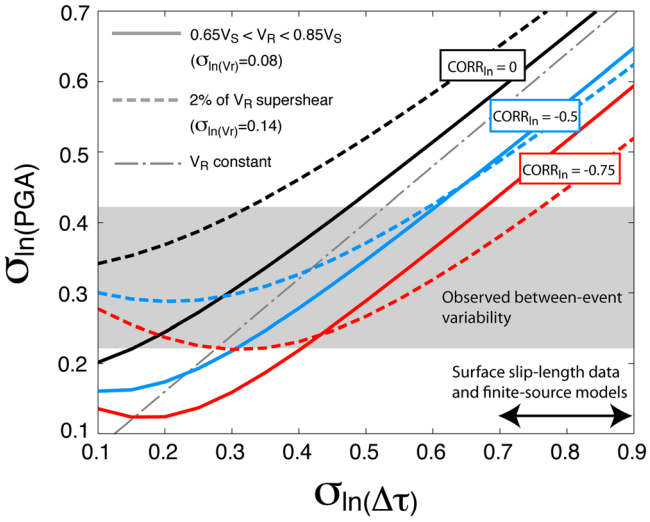

Figure 1. Variability of PGA computed from equation (4) as a function of the stress drop variability, considering various levels of correlation between stress drop and rupture velocity ($CORR_{ln}$ denotes the coefficient of correlation between $\ln(V_r)$ and $\ln(\Delta\tau)$). The rupture velocity is assumed to be subshear, uniformly distributed in the range [$0.65V_S$–$0.85V_S$] (solid line), or include 2% of supershear ruptures (dashed line). For comparison, the gray line indicates the PGA variability assuming a constant rupture velocity ($\sigma_{\ln(PGA)} = 0.8\sigma_{\ln(\Delta\tau)}$). The gray horizontal bar represents the range of observed between-event variability of PGA (Table 2).

explain this overestimation: either $\sigma_{\ln(\Delta\tau)}$ is smaller than 0.7, or $\Delta\tau$ and V_r are anticorrelated ($CORR_{ln} < 0$). Decreasing $\sigma_{\ln(\Delta\tau)}$ up to ~0.5 results in $\sigma_{\ln(PGA)} >$ ~0.45, which is still above the reported PGA between event variability so that the first hypothesis alone does not explain the low PGA variability. The second hypothesis may help to resolve this inconsistency. We suggest that there is a significant level of anticorrelation between $\Delta\tau$ and V_r ($CORR_{ln} < -0.5$).

4. Validation in the Case of 1-D Heterogeneous Ruptures

The validity of equation (4) is checked in the case of simple heterogeneous ruptures. We deploy a 1-D stochastic source model in which the amplitude spectrum of the final slip follows a k^{-2} asymptotic decay beyond $k = 1/L$, where L is the fault length [*Bernard et al.*, 1996]. The phases of the slip spectrum are randomly chosen. The rupture is supposed to propagate unilaterally (as observed for most earthquakes) [*McGuire et al.*, 2002] and at a constant rupture velocity so that the generated ground displacement spectra match the commonly observed ω^{-2} *Brune's* [1970] model.

We remind the reader that our study focuses on the variability of PGA and not its absolute value. In addition, we analyze the dependence of the PGA variability on $\Delta\tau$ and V_r only so that path effects and directivity effects are fixed. Hence, we assume that the radiated source energy propagates in a homogeneous infinite elastic medium and at a fixed azimuth. The far-field ground acceleration can then be simply computed as [e.g., *Aki and Richards*, 2002]

$$\ddot{u}(t,r) = \gamma \dddot{M}\,(t - r/V_b) \tag{7}$$

where γ is a constant depending on the radiation pattern of the considered body wave, the distance to the source, the density, the wave velocity V_b, and $\dot{M}(t)$ is the moment rate function. Note that the far-field approximation is adequate because the observations of PGA between-event variability mainly arise from

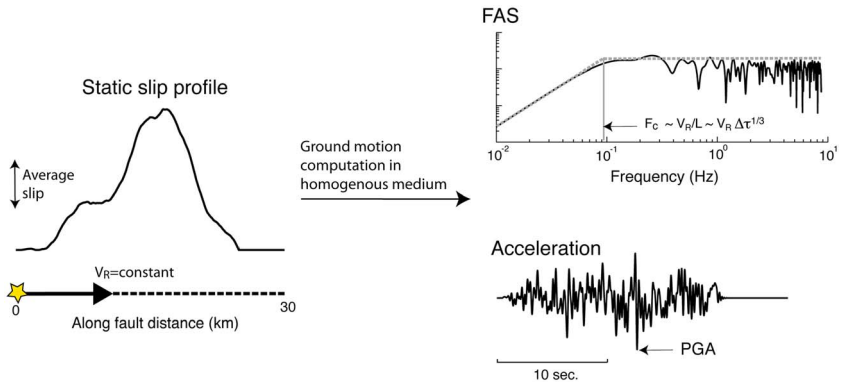

Figure 2. (a) Example of static slip distribution generated from the 1-D stochastic source model, (b) resulting Fourier acceleration spectrum, and (c) acceleration time history computed using equation (7). The example is for a rupture length $L = 30$ km, $V_r = 2600$ m/s and a source receiver azimuth of 90°.

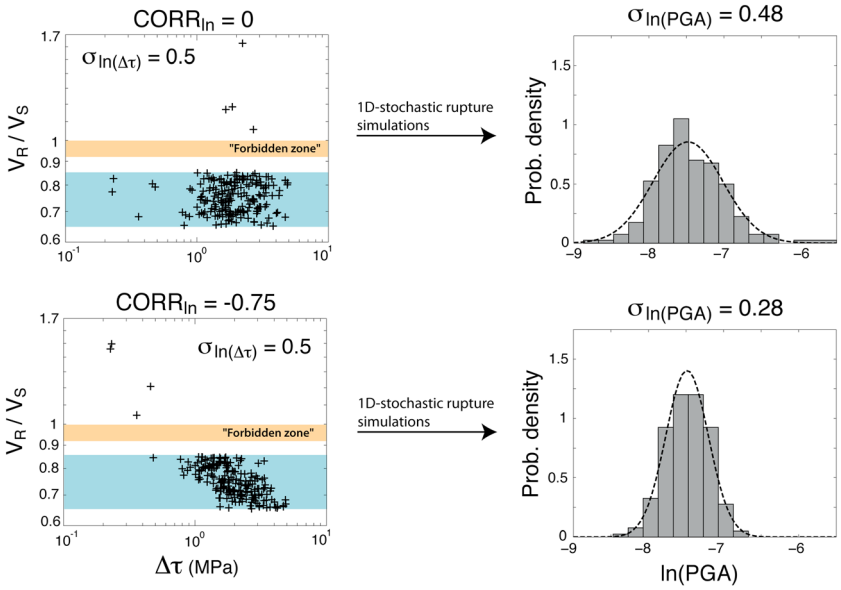

Figure 3. (left) distribution of stress drop ($\sigma_{\ln(\Delta\tau)} = 0.5$) and rupture velocity (uniform in the range [$0.65V_s$–$0.85V_s$] but assuming 2% are supershear) for different levels of correlations ($CORR_{ln}$ is the coefficient of correlation between $\ln(V_r)$ and $\ln(\Delta\tau)$). (right) Resulting distribution of PGA computed using the 1-D stochastic source model.

far-field strong motion data. An example of generated slip distribution and resulting acceleration time history and Fourier amplitude spectrum is presented in Figure 2. Note that the 1-D approximation (line source) does not account for slip fluctuations on a 2-D fault plane but correctly represents the average rupture velocity, the average stress drop, and the far-field predicted acceleration.

Figure 3 shows the distributions of $\Delta\tau$ and V_r (left) considering $\sigma_{\ln(\Delta\tau)} = 0.5$ with $CORR_{ln} = 0$ (top) and $CORR_{ln} = -0.75$ (bottom), and the distributions of PGA obtained from the 1-D stochastic source model (right). The resulting values of $\sigma_{\ln(PGA)}$ (0.48 for $CORR_{ln} = 0$ and 0.28 for $CORR_{ln} = -0.75$) match fairly well the assumed $\sigma_{\ln(PGA)}$ from Figure 1 and equation (4) (0.52 for $CORR_{ln} = 0$ and 0.27 for $CORR_{ln} = -0.75$), indicating that the source features of unilateral 1-D heterogeneous ruptures are captured by equation (4).

5. Discussion

Our study suggests that $\Delta\tau$ and V_r are not independent but anticorrelated. The inferred level of anticorrelation strongly depends on the value of $\sigma_{\ln(\Delta\tau)}$. If $\sigma_{\ln(\Delta\tau)} \sim 0.7$ as reported by several recent analyses of slip-length surface observations and finite-source rupture models (see Table 1), it is likely that the coefficient of correlation between $\ln(V_r)$ and $\ln(\Delta\tau)$, $CORR_{ln}$, is smaller than -0.75. If $\sigma_{\ln(\Delta\tau)}$ is smaller, for instance $\sigma_{\ln(\Delta\tau)} \sim 0.5$, $CORR_{ln}$ may be on the order of -0.5 to be consistent with observations of PGA between-event variability. The following questions remain: what part of the variability in $\Delta\tau$ actually arises from the natural randomness of the source process, and what part is due to uncertainties?

Slip-length surface data have the advantage of being direct geological observations. *Wells and Coppersmith* [1994] claim that uncertainty in surface rupture length in their database is less than 20%. Uncertainty in the maximum slip (D_{max}) or average slip (D_{mean}) may be larger due to the limited number of measurement points along the rupture. In order to get an approximation of this uncertainty, we consider the surface slip profile of the 1940 Imperial Valley earthquake obtained by *Rockwell and Klinger* [2013] using high-resolution aerial photography. This is one of the best sampled surface rupture that has been obtained so far, with ~630 measurements of displacement along a 15 km fault segment (Figure S1 in the supporting information). Taking random subsamples of 35 points (as was approximately the case in former studies), we obtain that the standard deviation of the natural logarithm residuals is 0.12 for D_{max} and 0.17 for D_{mean}. Measurement uncertainty in slip-length surface data seems thus to be negligible with respect to the reported variability of D_{max}/L or D_{mean}/L (~0.7). Nevertheless, D_{max}/L and D_{mean}/L obtained at surface are not direct estimations

of the stress drop as defined in equation (6). First, observations at surface do not necessarily map the rupture process at depth. Second, stress drop depends on the 2-D source geometry. *Noda et al.* [2013] have shown that coefficient C in equation (6) increases from 2.5 to 5.2 for rectangular ruptures with aspect ratios of 1 and 16, respectively. It is difficult to determine whether the variability of D_{max}/L and D_{mean}/L is smaller or larger than the actual stress drop variability.

On the contrary to slip-length surface data, finite-source rupture models account for the 2-D source geometry by providing the spatial slip distribution. Such source models are obtained by means of inversion techniques, using strong motion, teleseismic, GPS, and/or interferometric synthetic aperture radar data. Several studies have shown that the details of the slip distribution cannot be resolved due to large uncertainties in inversion techniques [e.g., *Mai et al.*, 2007]. *Causse et al.* [2014] find that the uncertainty in average stress drop associated with uncertainties in various finite-source rupture models remains, however, on the order of 0.15, which is also much smaller than the reported stress drop variability (~0.7).

Therefore, we claim that the reported variability of stress drop $\sigma_{\ln(\Delta\tau)}$ (Table 1) mainly reflects the natural source randomness.

Our results imply that ruptures that propagate rapidly have preferentially low stress drop. This is consistent with the observation that most of the observed supershear ruptures occurred on "mature" faults, which are generally associated with low stress drop [*Manighetti et al.*, 2007] and usually produce low PGA [*Bouchon and Karabulut*, 2008]. Besides, evidence of ruptures with small stress drop propagating faster has also been reported in the case of subshear ruptures by *Tan and Helmberger* [2010] from the 2003 Big Bear sequence ($3 < M < 5$).

Finally, it is important to note our 1-D stochastic source model assumes a constant rupture velocity, whereas PGA generated by real earthquakes may be affected by fluctuations of the local rupture velocity. Besides, in addition to the shape of the Fourier spectrum, which describes the correlation structures of source parameters, the PGA variability may also be affected by the variability of the slip at a given location (e.g. *Lavallée and Archuleta* [2005], *Song and Dalguer* [2013]).

6. Conclusion

The variability of PGA depends on the variability of $\Delta\tau$ and V_r and the correlation between the two. By considering the variability of $\Delta\tau$ and V_r consistent with several recent source studies, we have shown that the hypothesis of independency between $\Delta\tau$ and V_r gives rise to an overestimation of the variability of PGA between-event terms. This indicates that $\Delta\tau$ and V_r are likely anticorrelated. We found that the correlation is significant, with $CORR_{ln} < \sim -0.5$. Further investigations of the probability density functions of $\Delta\tau$, V_r, and PGA may help to refine the correlation estimate. Our study shows that joint probability distributions of stress drop and rupture velocity should be considered in ground motion prediction. It also points out the need of independent and robust estimates of stress drop and rupture velocity of earthquakes to properly quantify the correlation and to understand the physical underlying processes.

Acknowledgments

The authors thank Annemarie Baltay and an anonymous reviewer, whose comments greatly improved the paper. The authors also thank François Renard and Bruce Shaw for helpful comments and Yan Klinger for providing the 1940 Imperial Valley surface slip profile. All other data used in this paper are derived from published sources in the references. This work was in part supported by the Basic Research Project of Korea Institute of Geoscience and Mineral Resources (KIGAM), funded by the Ministry of Science, ICT & Future Planning (MSIP, Korea).

The Editor thanks Annemarie Baltay and an anonymous reviewer for their assistance in evaluating this paper.

References

Abrahamson, N. A., W. J. Silva, and R. Kamai (2014), Summary of the ASK14 ground motion relation for active crustal regions, *Earthquake Spectra*, *30*, 1025–1055.

Aki, K., and P. G. Richards (2002), *Quantitative Seismology*, 2nd ed., Univ. Science Books, Sausalito, Calif.

Akkar, S., and J. J. Bommer (2010), Empirical equations for the prediction of PGA, PGV and spectral accelerations in Europe, the Mediterranean and the Middle East, *Seismol. Res. Lett.*, *81*, 195–206.

Al-Atik, L., N. Abrahamson, J. J. Bommer, F. Scherbaum, F. Cotton, and N. Kuehn (2010), The variability of ground-motion prediction models and its components, *Seismol. Res. Lett.*, *81*, 794–801.

Allmann, B., and P. Shearer (2009), Global variations of stress drop for moderate to large earthquakes, *J. Geophys. Res.*, *114*, B01310, doi:10.1029/2008JB005821.

Anderson, J. G., and J. N. Brune (1999), Probabilistic seismic hazard assessment without the ergodic assumption, *Seismol. Res. Lett.*, *70*, 19–28.

Andrews, D. J. (1976), Rupture velocity of plane strain shear cracks, *J. Geophys. Res.*, *81*, 5679–5687, doi:10.1029/JB081i032p05679.

Baltay, A. S., T. C. Hanks, and G. C. Beroza (2013), Stable stress-drop measurements and their variability: Implications for ground-motion prediction, *Bull. Seismol. Soc. Am.*, *103*, 211–222.

Bernard, P., A. Herrero, and C. Berge (1996), Modeling directivity of heterogeneous earthquakes ruptures, *Bull. Seismol. Soc. Am.*, *86*, 1149–1160.

Bizzarri, A., and S. Das (2012), Mechanics of 3-D shear cracks between Rayleigh and shear wave rupture speeds, *Earth Planet. Sci. Lett.*, *357–358*, 397–404.

Bommer, J. J., et al. (2004), The challenge of defining upper bounds on earthquake ground motions, *Seismol. Res. Lett.*, *75*, 82–95.
Boore, D. (1983), Stochastic simulation of high-frequency ground motions based on seismological models of the radiated spectra, *Bull. Seismol. Soc. Am.*, *73*, 1866–1894.
Boore, D. M., J. P. Stewart, E. Seyhan, and G. A. Atkinson (2014), NGA-West2 equations for predicting PGA, PGV, and 5% damped PSA for shallow crustal earthquakes, *Earthquake Spectra*, *30*, 1057–1085.
Bouchon, M. (1997), The state of stress on some faults of the San Andreas system as inferred from near-field strong motion data, *J. Geophys. Res.*, *102*, 11,731–11,744, doi:10.1029/97JB00623.
Bouchon, M., and H. Karabulut (2008), The aftershock signature of supershear earthquakes, *Science*, *320*, 1323–1325, doi:10.1126/science.1155030.
Bouchon, M., M. P. Bouin, H. Karabulut, M. Nafi Toksöz, M. Dietrich, and A. J. Rosakis (2001), How fast is rupture during an earthquake? New insights from the 1999 Turkey earthquakes, *Geophys. Res. Lett.*, *14*, 2723–2726, doi:10.1029/2001GL013112.
Brune, J. N. (1970), Tectonic stress and the spectra of shear waves from earthquakes, *J. Geophys. Res.*, *75*, 4997–5009, doi:10.1029/JB075i026p04997.
Campbell, K. W., and Y. Bozorgnia (2014), NGA-West2 ground motion models for the horizontal average componets of PGA, PGV, and 5% damped linear acceleration response spectra, *Earthquake Spectra*, *30*, 1087–1115.
Causse, M., L. A. Dalguer, and P. M. Mai (2014), Variability of dynamic source parameters inferred from kinematic models of past earthquakes, *Geophys. J. Int.*, *196*, 1754–1769.
Chiou, B. S.-J., and R. R. Youngs (2014), Update of the Chiou and Youngs NGA model for the average horizontal component of peak ground motion and response spectra, *Earthquake Spectra*, *30*, 1117–1153.
Cotton, F., R. Archuleta, and M. Causse (2013), What is sigma of stress drop?, *Seismol. Res. Lett.*, *84*, 42–48.
Hanks, T. C. (1979), *b* values and ω-γ seismic source models: Implications for tectonic stress variations along active crustal fault zones and the estimation of high-frequency strong ground motion, *J. Geophys. Res.*, *84*(B5), 2235–2242.
Hanks, T. C., and R. K. McGuire (1981), Character of high-frequency strong ground motion, *Bull. Seismol. Soc. Am.*, *71*, 2017–2095.
Heaton, T. H. (1990), Evidence for and implications of self-healing pulses of slip in earthquake rupture, *Phys. Earth Planet Int.*, *64*, 1–20.
Kanamori, H., and D. L. Anderson (1975), Theoretical basis of some empirical relations in seismology, *Bull. Seismol. Soc. Am.*, *65*, 1073–1095.
Kanamori, H., and L. Rivera (2004), Static and dynamic scaling relations for earthquakes and their implications for rupture speed and stress drop, *Bull. Seismol. Soc. Am.*, *94*, 314–319.
Kaneko, Y., and P. Shearer (2015), Variability of seismic source spectra, estimated stress drop and radiated energy, derived from cohesive-zone models of symmetrical and asymmetrical circular and elliptical ruptures, *J. Geophys. Res. Solid Earth*, *120*, 1053–1079, doi:10.1002/2014JB011642.
Lavallée, D., and R. J. Archuleta (2005), Coupling of random properties of the source and the ground motion for the 1999 Chi Chi earthquake, *Geophys. Res. Lett.*, *32*, L08311, doi:10.1029/2004GL022202.
Mai, P. M., and G. C. Beroza (2000), Source scaling properties from finite-fault-rupture models, *Bull. Seismol. Soc. Am.*, *90*, 604–615.
Mai, P. M., J. Burjanek, B. Delouis, G. Festa, C. Francois-Holden, D. Monelli, T. Uchide, and J. Zahradnik (2007), Source-inversion blindtest: initial results and further developments, *Eos Trans. AGU*, *88*(52), Fall Meet. Suppl., Abstract S53C-08.
Manighetti, I., M. Campillo, S. Bouley, and F. Cotton (2007), Earthquake scaling, fault segmentation and structural maturity, *Earth Planet. Sci. Lett.*, *253*, 429–438.
McGuire, J. J., L. Zhao, and T. H. Jordan (2002), Predominance of unilateral rupture for a global catalog of large earthquakes, *Bull. Seismol. Soc. Am.*, *92*(8), 3309–3317.
McGuire, R. K., and T. C. Hanks (1980), RMS accelerations and spectral amplitudes of strong motion during the San Fernando earthquake, *Bull. Seismol. Soc. Am.*, *70*, 1907–1920.
Noda, H., N. Lapusta, and H. Kanamori (2013), Comparison of average stress drop measures for ruptures with heterogeneous stress change and implications for earthquake physics, *Geophys. J. Int.*, *193*, 1691–1712.
Rockwell, T. K., and Y. Klinger (2013), Surface rupture and slip distribution of the 1940 Imperial Valley earthquake, Imperial fault, Southern California: Implications for rupture segmentation and dynamics, *Bull. Seismol. Soc. Am.*, *103*, 629–640.
Shaw, B. (2013), Earthquake surface slip-length data is fit by constant stress drop and is useful for seismic hazard analysis, *Bull. Seismol. Soc. Am.*, *103*, 876–893.
Song, S. G., and L. A. Dalguer (2013), Importance of 1-point statistics in earthquakesource modelling for ground motion simulation, *Geophys. J. Int.*, *192*, 1255–1270.
Tan, Y., and D. Helmberger (2010), Rupture directivity characteristics of the 2003 Bib Bear sequence, *Bull. Seismol. Soc. Am.*, *100*, 1089–1106.
Wells, D. L., and K. J. Coppersmith (1994), New empirical relationships among magnitude, rupture length, rupture width, rupture area, and surface displacement, *Bull. Seismol. Soc. Am.*, *84*, 974–1002.
Yue, H., T. Lay, J. T. Freymueller, K. Ding, L. Rivera, N. A. Ruppert, and K. D. Koper (2013), Supershear rupture of the 5 January 2013 Craig, Alaska (M_w 7.5) earthquake, *J. Geophys. Res. Solid Earth*, *118*, 5903–5919.